Interpretation of silica-disk-tests including the effect of limited mass transfer at the surface

Theo Fett, Günter Schell, Claudia Bucharsky
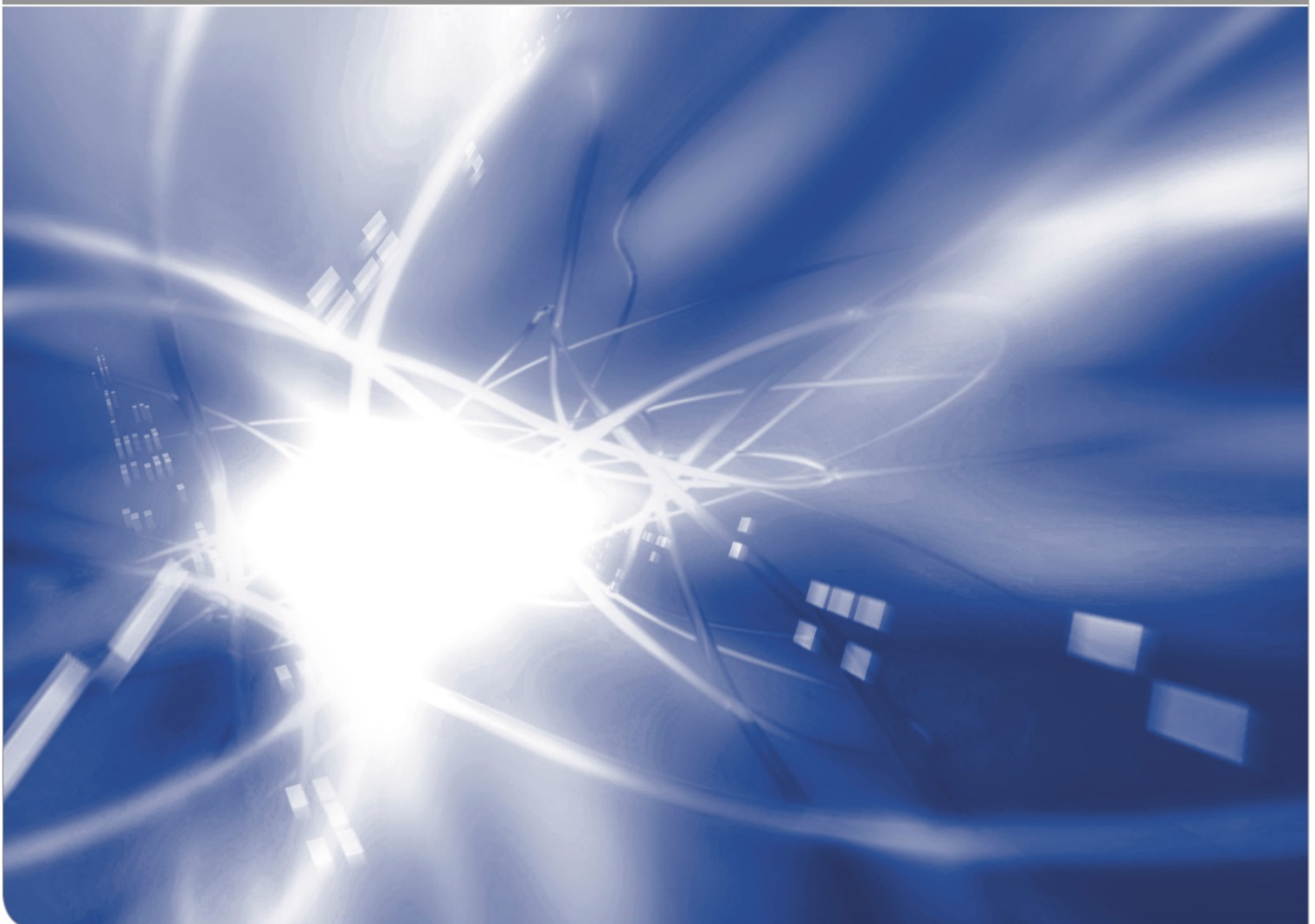
Institute for Applied Materials

Abstract

The concentration of water penetrated into silica depends strongly on the stress state in the surface region. In the water diffusion zone hydroxyl water is generated by the water/silica reaction that is at temperatures <450°C a first-order reaction. When [2*S*]=[2 SiOH] is the concentration of the immovable hydroxyl, the reaction equation reads

$$\equiv\text{Si-O-Si}\equiv +\text{H}_2\text{O} \leftrightarrow [2\text{ SiOH}]$$

When evaluating the deformation measurements on water-infiltrated silica disks, the question remained unanswered as to why the tests can lead to increased diffusion constants or whether these are accidental (possibly dependent on the special glass composition).

The result of this Report is:

- The activation volume for stress affected hydroxyl *S* is $\Delta V \cong 58$ cm^3/mol,

- the mass transfer coefficient of water into silica is $h/\sqrt{D} = 0.266/\sqrt{\text{h}}$,

- due to the mass transfer coefficient, the effective diffusivity is increased by a factor of roughly 1.6.

Contents

1 Basic equations

1.1 Water/silica reaction

Water penetrated into silica reacts with the silica network according to

$$\equiv\text{Si-O-Si}\equiv +\text{H}_2\text{O} \leftrightarrow \equiv\text{SiOH}+\text{HOSi}\equiv \qquad (1a)$$

with the concentration of the hydroxyl $S=[\equiv\text{SiOH}]$ and that of the molecular water $C=[\text{H}_2\text{O}]$. The equilibrium constant k of this reaction is at temperatures of $\theta<450°\text{C}$

$$k = \frac{S}{C} \qquad (2)$$

Water concentrations at silica surfaces under saturation pressure are available from investigations by Öhler and Tomozawa [1] and Zouine et al. [2]. Since the Zouine data [2] extend over the large temperature range of $23°\text{C}\leq\theta\leq200°\text{C}$, these results may be applied in the following considerations.

In *molar units*, the total water concentration is given by

$$C_w = C + \tfrac{1}{2}S = C(1+\tfrac{1}{2}k) \qquad (3)$$

The reaction volume ΔV can reach high values [3] for temperatures $<450°\text{C}$ and may be different in the temperature regions of $<450°\text{C}$ (first-order reaction) and $>450°\text{C}$ (second-order reaction).

When $[2S]=[2\ \text{SiOH}]$ is the concentration of the immovable hydroxyl, the reaction equation (1a) reads

$$\equiv\text{Si-O-Si}\equiv +\text{H}_2\text{O} \leftrightarrow [2\ \text{SiOH}] \qquad (1b)$$

In this case the reaction or activation volume is

$$\Delta V = \overline{V}_{[2S]} - \overline{V}_C . \qquad (4)$$

with the partial molar volume for [2 SiOH], denoted by $\overline{V}_{[2S]}$.

The hydroxyl S reads in *mass units*

$$S = \frac{17}{18}\frac{C_w}{\left(\dfrac{1}{2}+\dfrac{1}{k}\right)} \qquad (5)$$

1.2 Swelling stresses at 200°C

Due to the hydroxyl content S in the surface layer the glass will expand. This is suppressed by the bulk material. The consequence is a negative swelling stress σ_{sw}. In the absence of externally applied stresses, it holds for the hydrostatic stress term $\sigma_h = \sigma_{sw,h}$. Then the equilibrium constant reads according to [4]

$$k = k_0 \exp\left(\sigma_{sw,h}\frac{\Delta V}{RT}\right) = k_0 \exp\left(-\lambda\frac{S\Delta V}{RT}\right) \tag{6}$$

with $\lambda = 18.75$ GPa. k is the equilibrium constant, p is pressure, ΔV is the reaction volume, R is the universal gas constant and T is the temperature in °K.

A similar relation between stress and hydroxyl concentration holds for the equi-biaxial swelling stress components in the surface plane, namely,

$$\sigma_{sw,x,y} = -28\text{GPa} \times S, \; \sigma_{sw,z} = 0 \tag{7}$$

1.3 Mass transfer at 200°C under saturation pressure

Doremus showed in [5], that the surface condition for diffusion in vapor as the environment is given by

$$\frac{dC}{dz} = \frac{h}{D}(C - C_0) \quad \text{at} \; z=0, \tag{8}$$

where C_0 is the concentration of molecular water reached at $z=0$ and $t\rightarrow\infty$ and D the diffusivity. Following the suggestion by [5], for a slow surface reaction that limits the entrance of molecular water species, the parameter h in (8) may be interpreted as a *reaction parameter*. On the other hand, a simpler phenomenological description is possible by assuming that a barrier exists to the transport of water across the surface of the glass [4]. This barrier gives rise to a *mass transfer coefficient* for diffusion, which slows the passage of water into the glass.

Solution of the diffusion equation requires an appropriate boundary condition, very often chosen as constant surface concentration of molecular water:

$$C(z = 0,t) \equiv C(0) = C_0 = \text{constant} \tag{9}$$

As shown by Carslaw and Jaeger (Section 2.7 in [6]), the concentration for a semi-infinite body is given at the surface, $z=0$:

$$C(0, t) = C_0\left(1 - \exp\left[\frac{h^2}{D}t\right]\text{erfc}\left[h\sqrt{\frac{t}{D}}\right]\right), \tag{10}$$

that would for equilibrium constant k=const. result in

$$S(0, t) = C_0 k \left(1 - \exp\left[\frac{h^2}{D} t \right] \text{erfc}\left[h\sqrt{\frac{t}{D}} \right] \right), \tag{11}$$

The solution via Carslaw and Jaeger is exact under the condition, that the right-hand side would contain time-independent parameters, i.e. $k=k_0$=const. Since the equilibrium constant k varies with the swelling stress, eq.(6), the swelling stresses themselves depend on the S concentration, this requirement is of course violated. Nevertheless, an approximate analytical solution for the case of varying $k(S)$ can be obtained following the general procedure usual in perturbation theory. If we consider the equilibrium constant as the disturbance parameter, perturbation theory suggests to solve the problem for the case of $k=k_0$ and to insert the disturbance parameter $k(S)$ into this solution. In terms of the hydroxyl concentration S it holds

$$S(0, t) \cong S_0 \exp\left[-\frac{\lambda\Delta V}{RT} S(0,t) \right] \left(1 - \exp\left[\frac{h^2}{D} t \right] \text{erfc}\left[h\sqrt{\frac{t}{D}} \right] \right), \tag{12}$$

establishing an *implicit* equation with the unknown surface concentration $S(0,t)$ on both sides of (12). The implicit solution of (12) reads

$$S(0, t) \cong \frac{RT}{\lambda\Delta V} \text{PLog}\left[\frac{\lambda S_0 \Delta V}{RT} \left(1 - \exp\left[\frac{h^2}{D} t \right] \text{erfc}\left[h\sqrt{\frac{t}{D}} \right] \right) \right] \tag{13}$$

Temperature/ Exposure Time (θ / t)	Measured surface stress [10] (MPa)	Surface stress for θ=200°C (MPa)
196 °C/2.2h	-41.8	-36.
196 °C/20h	-46.9	-48.6
216 °C/20h	-50.3	-43.4
201 °C/96h	-54.7	-54.2
188 °C/168h	-53.5	-59.8

Table 1: Prediction of surface stresses using mass transfer parameter $h/\sqrt{t}$, [7].

In order to eliminate the temperature dependence, we computed the ratio $S(\theta)/S(200°C)$ and corrected the systematic influence of deviating temperatures according to Table 1 by

$$\sigma(200°C) \cong \frac{S(200°C)}{S(\theta)} \sigma(\theta) \tag{14}$$

3

2 Application on swelling data from silica disk experiments

2.1 Reaction volume and mass transfer from curve fitting

From the measurements of the swelling stresses and the associated layer thicknesses, it was found that their product agreed with the measured bending moments. The diffusivities were compared to the "standard diffusivities" according to Zouine et al. [2] slightly increased by about 60%. Consequently, the swelling stresses must have been about 30% too low. In addition to the glass swelling, this is to be interpreted as a consequence of the limited mass transfer (water in glass). In the present report, it is shown that the finite mass transfer coefficient must lead to an increase in the effective diffusion constant in the glass.

The swelling stresses transformed to $\theta=200°C$ are entered in the last column of Table 1 and shown in Fig. 1b. Next, we estimated the hydroxyl concentration for 200°C, Fig. 1b, from the disk-deformation measurements by Wiederhorn et al. [10] by fitting eqs.(7) and (13) to the surface swelling stresses, assuming the reaction volume ΔV and the mass-transfer coefficient $h/\sqrt{D}$ as the unknown parameters [8]. For this purpose, we applied the Mathematica-Procedure *FindFit* [9].
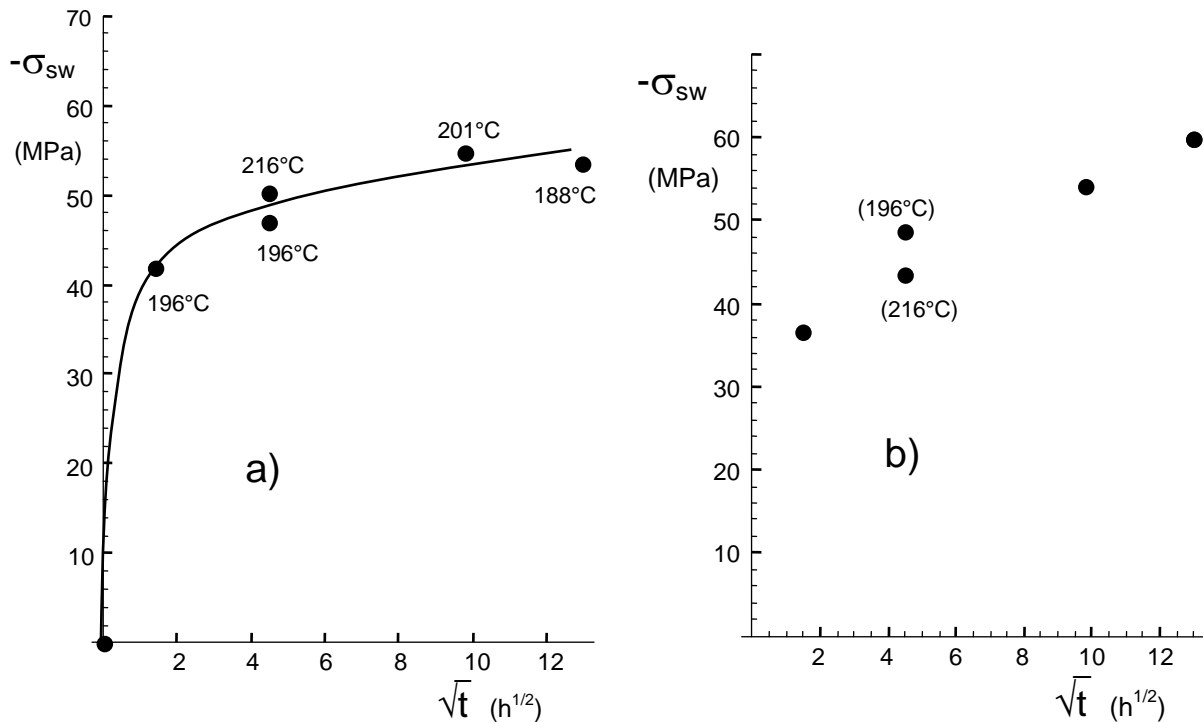
Fig. 1 Swelling stresses vs. soaking time in saturation water vapour, a) results from disk-deformations, reported in [10], b) data re-computed to constant temperature of $\theta=200°C$ using eq.(14).

Figure 2 shows the best fitting curve together with the experimental data of Fig. 1b in a plot with linear time scaling. The "best" set of parameters is

$$\Delta V \cong 57.8 \text{ cm}^3/\text{mol} \qquad (15a)$$

$$h/\sqrt{D} \cong 0.266 \text{ h}^{-1/2} \qquad (15b)$$

These parameters were used in the representation of Fig. 2a. The striking agreement between the calculated curve and the experimental data in Fig. 2a should not be over-estimated, as these measurements were used to derive the parameters ΔV and $h/\sqrt{D}$.
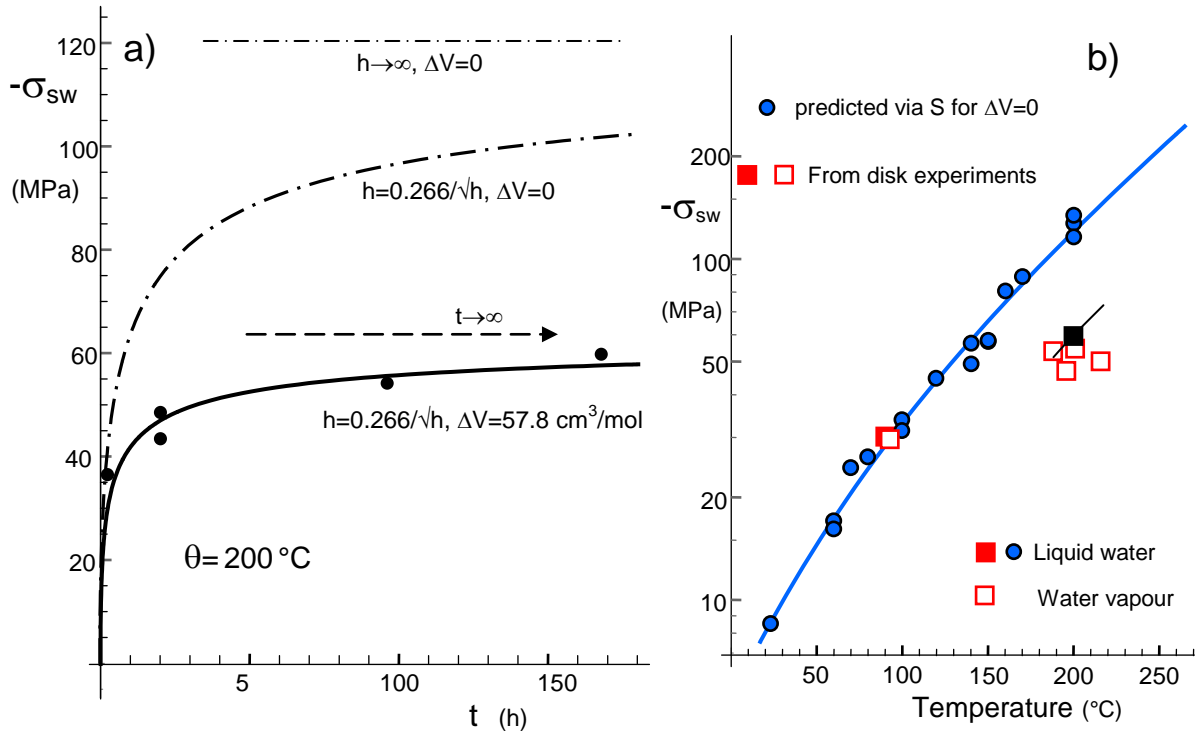
Fig. 2 a) Swelling stresses vs. time at 200°C. Circles: experimental results, curve: best fit by eq.(13), resulting in the parameter set of eqs.(15a, 15b), b) swelling stresses vs. temperature.

Different methods were used to determine the quantity $h/\sqrt{D}$ as a function of soaking temperature, especially at 200°C. In all cases, an effect of swelling on time-dependent surface concentrations was not yet taken into account. The red symbols indicate the mass-transfer coefficients $h/\sqrt{D}$ obtained from the water profiles by Helmich and Rauch [11] measured with the Nuclear Reaction Analysis (NRA). This technique provides a direct chemical analysis of the concentration of H as a function of distance from the specimen surface, here applied to depth $z=0$. An H-concentration fit of the

data by Helmich and Rauch [11] yields trivially the mass-transfer coefficient for the total water. In contrast to this, the disk deformations by Wiederhorn et al. [10] reflect the hydroxyl concentration S. It is hardly to be expected that these two properties are identical since they describe the behavior of different water species.

An equivalent representation of Fig. 1a is given in Figure 2b. Predictions under the assumption of $\Delta V=0$ are shown by the blue circles. The red squares indicate the experimental data of Fig. 1a with their slight deviations of test temperature from the nominal temperature of 200°C. The best fitting data, eqs.(15a, 15b) result in the black square, that was computed for a soaking time of $t\rightarrow\infty$ ($\sigma_{sw}\cong-63$ MPa, indicated by the dashed arrow).

Finally, the mass transfer coefficient $h/\sqrt{D}$ is introduced in Fig. 3 as the black square. This result is in agreement with transfer coefficients reported in [7].
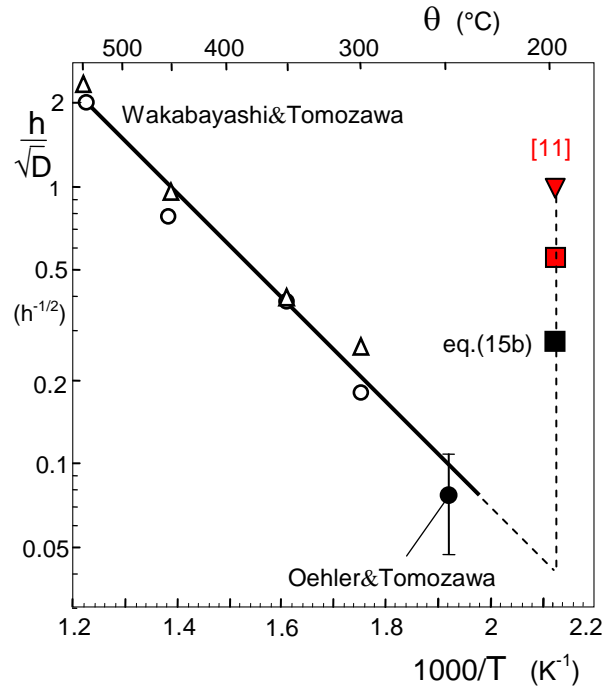
Fig. 3 Mass transfer parameter $h/\sqrt{D}$ as a function of temperature from [7]. Additionally plotted: black square: result of eq.(15b) for the disk glass in [10]. Red symbols: From results by Helmich and Rauch [11], evaluated in [7].

2.2 Apparent diffusivity

So far, we only considered the surface value of hydroxyl water and swelling strains. In addition to the swelling stresses, the disk measurements also revealed the diffusion constant [10].

Now let us look for their distribution over the surface region. As shown by Carslaw and Jaeger [6], the concentration profile, $C(z)$ resulting from the boundary condition for a *semi-infinite* body is given by

$$C(z, t)/C_0 = \text{erfc}\left[\frac{z}{2\sqrt{Dt}}\right] - \exp\left[\frac{h}{D}z + \frac{h^2}{D}t\right]\text{erfc}\left[\frac{z}{2\sqrt{Dt}} + h\sqrt{\frac{t}{D}}\right] \qquad (16)$$

For $h/\sqrt{D}$ we use eq.(15b) and for the diffusivity $D_{200°C}$ it results from Zouine et al. [2] $D_{200°C}=8\times10^{-17}$ m^2/s. By using the same strategy as leading to eq.(13), we obtain

$$S(z, t) \cong \frac{RT}{\lambda\Delta V}\text{PLog}\left[\frac{\lambda S_0 \Delta V}{RT}\left(\text{erfc}\left[\frac{z}{2\sqrt{Dt}}\right] - \exp\left[\frac{h}{D}z + \frac{h^2}{D}t\right]\text{erfc}\left[\frac{z}{2\sqrt{Dt}} + h\sqrt{\frac{t}{D}}\right]\right)\right] \quad (17)$$

Figure 4a illustrates the solution of the hydroxyl water S computed via eq.(17). With increasing swelling, i.e. increasing reaction or activation volumes ΔV, the maximum concentrations decrease and the half widths increase. Whereas for ignored swelling, $\Delta V=0$, the half-widths is ≈4.5 μm, it becomes ≈6 μm for the "best data set" of eqs.(15a) and (15b). An increase of roughly 33% is shown in Fig. 4b where the ratio of the thicknesses in presence and in the absence of swelling is plotted as a function of the activation volume ΔV. Since the layer thickness is proportional to square-root of time, $b\propto\sqrt{t}$, the ratio of the diffusivities result as shown in Fig. 4c.
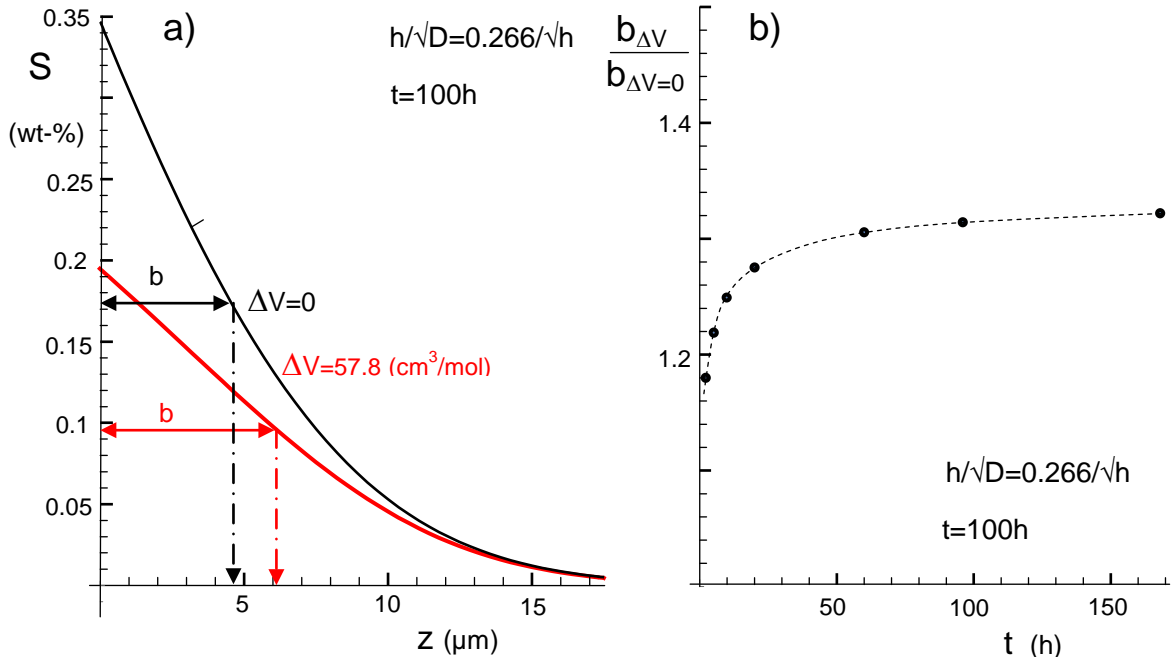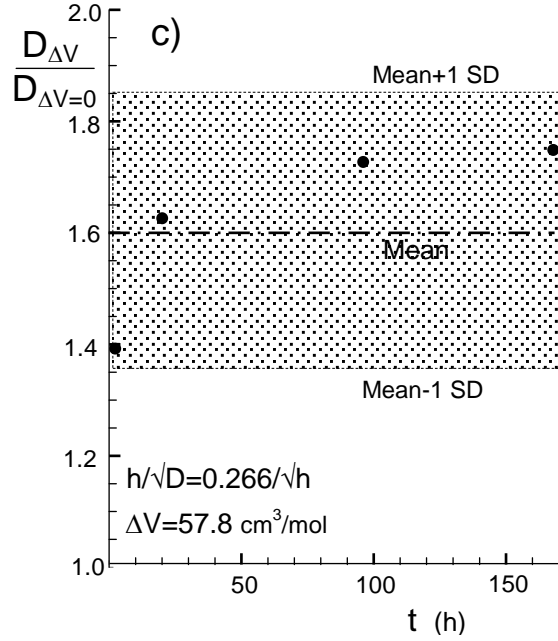
Fig. 4 a) Hydroxyl profiles for $h/\sqrt{D}=0.27/\sqrt{h}$ and different activation volumes ΔV, b) ratio of the swelling-affected *S*- layer thickness $b_{\Delta V}$ to the diffusivity in the absence of swelling, $\Delta V=0$, b) ratio of the swelling-affected diffusivity $D_{\Delta V}$ to the diffusivity in the absence of swelling, $\Delta V=0$. Additionally introduced is the result from the experiments in Table 2 (mean ratio and the standard deviation).

2.3 Comparison of computed and measured diffusivities

The experimental diffusivity data are compiled in Table 2. Figure 5a shows these results as red squares in comparison to the extensive measurements by Zouine et al [7] for liquid water as the surrounding medium. The latter were represented by the fitting equation

$$D = D_0 \exp[-Q/RT] \tag{18}$$

with D_0=7.6×10^{-5} (cm^2/s) and Q=72.3 kJ/mol. The data from Wiederhorn et al. [10] are given in column 2. The related diffusivities computed from (18) are listed in column 3 and their ratio in column 4.

The data we are interested in is in the dashed rectangle in the upper left corner. This area is reproduced in detail in Fig. 5b. The measured diffusivity values according to Wiederhorn et al. are drawn as squares. The straight line of the same slope, shifted by a factor of 1.6, is shown as a solid line and the scatter range of ± 1 standard deviation is shown as dashed lines.

Having in mind the high magnification of Fig. 5b, it is reasonable to conclude that the shift in the diffusion data is caused by mass transfer and swelling. Measured and computed shifts of 1.599 and 1.65, respectively, are in best agreement.

8

Temperature/ Time (θ/t)	Diffusivity via disk measurement [10] (cm²/s)	Diffusivity in liquid water [2], eq.(18)	$D([10])/D([2])$
196 °C/2.2h	1.27×10^{-12}	0.67×10^{-12}	1.895
196 °C/20h	1.19×10^{-12}	0.67×10^{-12}	1.776
216 °C/20h	1.97×10^{-12}	1.44×10^{-12}	1.368
201 °C/96h	1.36×10^{-12}	0.82×10^{-12}	1.658
188 °C/168h	0.636×10^{-12}	0.49×10^{-12}	1.298
Mean			1.599
1 SD.			0.258

Table 2: Diffusivities from disk deformations, [10], compared with measurements in liquid water, reported by Zouine et al. [2].
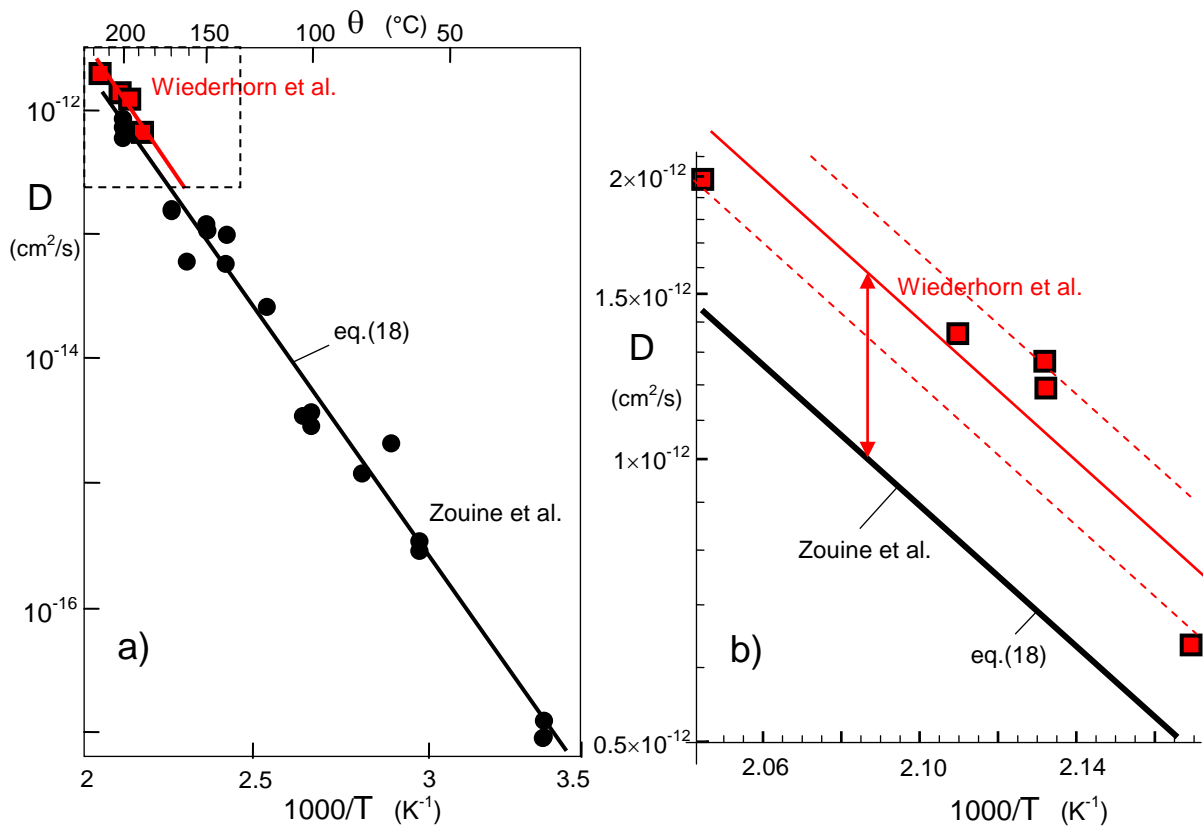
Fig. 5 Diffusivities; a) black circles: results for silica soaked in *liquid water* under saturation pressure by Zouine et al. [2], red symbols: from disk deformations after soaking in *water vapour* of saturation pressure, b) details in the dashed rectangle of Fig. 5a.

References

1 Oehler, A., Tomozawa, M., Water diffusion into silica glass at a low temperature under high water vapor pressure, J. Non-Cryst. Sol. **347**(2004) 211-219.

2 A. Zouine, O. Dersch, G. Walter and F. Rauch, "Diffusivity and solubility of water in silica glass in the temperature range 23-200°C," *Phys. Chem. Glass: Eur. J. Glass Sci and Tech. Pt. B*, **48** [2] 85-91 (2007).

3 G. Schell, G. Rizzi, T. Fett, Hydroxyl concentrations on crack surfaces from measurements by Tomozawa, Han and Lanford, Scientific Working Papers SWP **82**, 2018, ISSN: 2194-1629, Karlsruhe, KIT.

4 T. Fett, G. Rizzi, K.G. Schell, C.E. Bucharsky, P. Hettich, S. Wagner, M. J. Hoffmann, Consequences of hydroxyl generation by the silica/water reaction, Part I: Diffusion and Swelling, KIT Scientific Publishing, **101**(2022), Karlsruhe.

5 R.H. Doremus, Diffusion of Reactive Molecules in Solids and Melts, Wiley, 2002, NewYork.

6 Carslaw, H.S., Jaeger, J.C. Conduction of heat in solids, 2nd ed. 1959, Oxford Press, London.

7 T. Fett, K. G. Schell, C. Bucharsky, Mass Transfer of Water at Silica Surfaces - Extension of the data base to lower temperatures, Scientific Working Papers SWP **189**, 2022, ISSN: 2194-1629, Karlsruhe, KIT.

8 T. Fett, K. G. Schell, C. Bucharsky, Distribution of equilibrium constant k and hydroxyl S in silica surface layers, Scientific Working Papers SWP **195**, 2022, ISSN: 2194-1629, Karlsruhe, KIT.

9 *Mathematica*, Wolfram Research, Champaign, USA.

10 S. M. Wiederhorn, F. Yi, D. LaVan, T. Fett, M.J. Hoffmann, Volume Expansion caused by Water Penetration into Silica Glass, J. Am. Ceram. Soc. **98** (2015), 78-87.

11 M. Helmich and F. Rauch, On the mechanism of diffusion of water in silica glass, *Glastech. Ber.* **66** [8] (1993), 195-200.